Intrinsic Defects in Strontium Aluminates studied via Computer Simulation Technique

M V dos S Rezende[1,3],**R M Araujo**[1], **M E G Valerio**[1] and **R A Jackson**[2]

[1]Physics Department, Federal University of Sergipe, Campus Universitário, 491000-000 São Cristovão-SE, Brazil

[2]School of Physical and Geographical Sciences,, Keele University, Keele, Staffordshire, UK ST5 5BG

E-mail: mvsrezende@gmail.com, mvalerio@ufs.br

Abstract. We present the results of computer simulation studies for all 10 different crystalline phases of the strontium aluminate family. After deriving a reliable potential model that reproduces all structures, the energetic process involving in creation of intrinsic defects were calculated, namely the Schottky, pseudo-Schottky, anti-Schottky, and Frenkel defects. The results indicated that the entire family of strontium aluminates can be divided in three groups according to the type of the predominant intrinsic defect formed, SrO pseudo-Schottky defect, oxygen Frenkel defect or Strontium Frenkel defect.

1. Introduction

Strontium aluminates have been studied because of its interesting structural and optical properties. Several of these compounds have long lasting phosphorescence for more than 1 h, when doped with trivalent and divalent rare-earth ions [1]. Results reported in the literature showed that $SrAl_2O_4:Eu^{2+},Dy^{3+},B^{3+}$, $Sr_4Al_{14}O_{25}:Eu^{2+},Dy^{3+},B^{3+}$[2], $SrAl_4O_7:Eu^{2+},Dy^{3+}$[3], $SrAl_{12}O_{19}: Eu^{2+}$, $Sr_2Al_6O_{11}$: Eu^{2+} [4], have a wide range of emission colors. Potential applications of these new phosphors are numerous, especially in the areas of safety improvement and energy saving (e.g., traffic signs, emergency signs, safety clothes, advertising, etc.).

Phosphorescence (or sometimes also confused with afterglow) refers to the light emission of an insulator that persists at room temperature after stopping excitation (usually UV irradiation). This delayed light emission is caused by the trapping of photo-generated electrons and/or holes at intrinsic or extrinsic defect sites of the material [5,6].

Computer simulation is a useful tool that can provide information on the relative energetic stability of different intrinsic and extrinsic defects, which, in turn, is a strong indication of the most probable one. As a consequence, this information can be used to explain the phosphorescence mechanisms. For example, the phosphorescence mechanism for $SrAl_2O_4:Eu^{2+}, Dy^{3+}, B^{3+}$ proposed by Clabau et al. [1] admits that, under UV irradiation, electrons are promoted from the occupied 4f levels of Eu^{2+} to the empty 5d levels and from the top of the valence band to the unoccupied 4f levels of residual Eu^{3+}, a kind of charge transfer mechanism. The Eu^{2+} electrons promoted to the 5d levels, that supposedly are located in the conduction band of the solid, can be trapped at oxygen vacancy (V_O) defects located in the vicinity of the photogenerated Eu^{3+} cations. The accompanying holes created in the valence band

---

[3]   To whom any correspondence should be addressed.

can be trapped at Sr or Al vacancy (V_{Sr} or V_{Al}) levels. This proposed mechanism is very dependent on the existence of different stable defects in the $SrAl_2O_4$ matrix, both from intrinsic and extrinsic origin and the existence of that defects are admitted by the authors without any further background.

The aim of the present work is to study all types of intrinsic defect, Frenkel, Schottky, pseudo-Schottky and anti-Schottky type defects, calculating the energetic of the production and stabilization of such defects in all strontium aluminates crystalline family.

Computer modelling methods employed in this work are based initially on well established approaches that use interatomic potentials to represent the interactions between the ions, coupled with energy minimization and Mott-Littleton methods to calculate the properties of 'pure' and the defective materials. In the first step, we obtained the potential parameters through the empirical fitting methods. In the second step, this potential set was used to model the intrinsic defects in all crystalline phases, ranging from Schottky, Pseudo-Schottky, Anti-Schottky, and Frenkel defects.

2. Structural information

The strontium aluminates compounds present different crystallographic forms depending of the ratio $SrO:Al_2O_3$. $Sr_4Al_{14}O_{25}$[7] and $Sr_2Al_6O_{11}$[8] exist in orthorhombic phase, while the $Sr_3Al_2O_6$[9] and $Sr_9Al_6O_{18}$[10] exists in cubic phase. The hexagonal phase is observed in $Sr_7Al_{12}O_{25}$[11] and $SrAl_{12}O_{19}$[12], and monoclinic phase is observed for $SrAl_4O_7$[13] and $Sr_{10}Al_6O_{19}$[14].

The $SrAl_2O_4$ exists in two crystallographic forms, and a reversible phase transition between the two occurs at 650°C (923K). At low temperature the monoclinic phase is observed [15] while at high temperature a hexagonal phase is observed [16]. There are two crystallographic non equivalent sites for Sr^{2+} in the monoclinic phase and three crystallographic non equivalent sites for Sr^{2+} in the hexagonal phase. The Sr^{2+} and rare earth ions are very similar in their ionic size (i.e., 1.21 and 0.86 to 0.96 Å, respectively) thus one would expect that the Sr^{2+} sites are the preferable sites for incorporation of the rare earth dopants.

Figures 1 and 2 show schematic representations of the $SrAl_2O_4$ phases. It can be seen that the Al tetrahedrons in hexagonal phase are more organized than in the monoclinic phase. The Al sites are almost perfect tetrahedral coordinated in the monoclinic phase while in the hexagonal phase the tetrahedral are slightly distorted. Thus the phase transition from monoclinic to hexagonal phase involves an organization of the special arrangement of the ions in the crystalline structure.
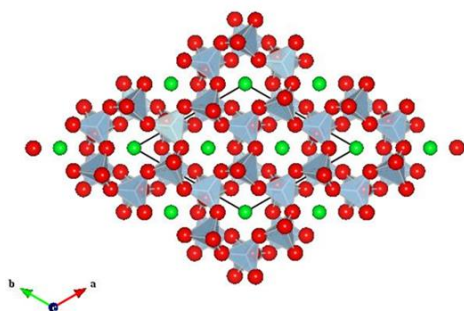

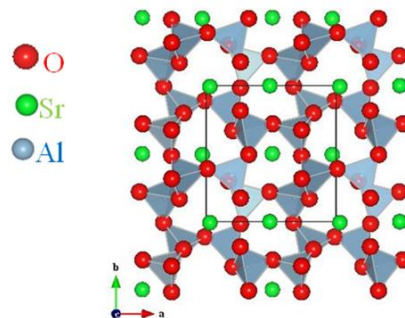Figure 1 – hexagonal phase $SrAl_2O_4$.   Figure 2 – monoclinic phase $SrAl_2O_4$.

3. Methodology

3.1. Derivation of potentials

The computational method used in the present work admits that any ionic material can be described in terms of ions interacting through effective potentials. Having specified these potentials, the lattice

energy of the material is minimized by varying the structural parameters (atomic positions and unit cell constants). The interatomic potentials used in this paper were obtained using empirical fitting methods as embodied in the GULP code [17]. The Buckingham potentials supplemented by electrostatic interaction terms, was used here since it successfully describes ion interaction in a huge variety of materials, as below

$$V(r_{ij}) = A_{ij} \exp(-r_{ij}/\rho_{ij}) - C_{ij} r_{ij}^{-6} + q_i q_j / r_{ij} \tag{1}$$

here q_i , q_j are charges on ions i and j, and A, ρ, and C are parameters whose values have to be obtained for each ion pair. The short range term, described by the first two terms in equation (1), are important to mimic two important non-Coulombic interactions: i-the repulsion due to superposition of the electronic clouds of the pair of ions related to the Pauli exclusion principle, sometimes called as Pauli repulsion, and ii-attractive terms due to polarization of the ions and other quantum attractive terms like exchange interactions.

Other important aspect of the modelling strategy is the explicit inclusion of the O^{2-} polarisability via the Shell Model, as proposed by Dick and Overhasuser [18]. This model considers that the polarisable specie is divided between a core that concentrates the mass of the ion and a shell coupled by a mass less spring constant. The charge of the ion is divided between the core and the shell. This model adds two extra parameters per polarisable ion, the spring constant and the shell charge. The short range terms act between the O^{2-} shells or between O^{2-} shells and the Sr^{2+} or Al^{3+} ions. The cations were considered rigid ions in the present work.

The short range potential parameters plus the shell model parameters for the anion were obtained by manual fitting to the structural properties of all strontium aluminate crystalline phases, and the result of that can be seen in table 1. During the fitting procedure, only the potentials parameters for the Sr-O and Al-O interactions were varied. The O-O interaction was held fix following Catlow et al [19]. Table 2 gives the comparison between the experimental and calculated lattice parameters. The structural parameters were evaluated at temperatures where each material was measured, according to the reference quoted on the table. The temperature effect is included in the GULP package based on the harmonic approximation [20]. It can be seen that the potential parameters are quite successfully on reproducing all the crystalline structures within 3%.

Table 1. Potential parameters, shell model constants and ionic charges obtained during the fitting to the structure of all strontium aluminate phases.

Interacion	A(eV)	ρ(Å)	C(eV.Å^6)	Cutoffs(Å)
Sr_{core}-O_{Shell}	1449.0	0.3427	0.00	10.0
Al_{core}-O_{Shell}	1235.3	0.3109	0.00	10.0
O_{shell}-O_{Shell}	22764.0	0.1490	27.88	10.0
Spring				
O_{core}-O_{Shell}	70.0	-	-	-
Charge	Z_{Sr}	Z_{Al}	Z_{Ocore}	Z_{Oshell}
	2.00	3.00	0.900	-2.900

The lattice energy and the lattice energy per ion of each of the strontium aluminate phases were calculated at 0K and 300K and they are shown in table 3. These values can be used to estimate the relative stability of each of these phases and it is shown from the energetic point of view that the most stable phase would be $SrAl_{12}O_{19}$. Comparing the two $SrAl_2O_4$ phases, it is shown that there is practically no difference between their lattice energies indicating that these two phases may coexist. This result is consistent with the experimental finds by Montes et al [21] that reports the existence of these two phases in their samples.

Table 2. Comparison of calculated and experimental structures.

Aluminates	Ref.	Parameter	Experimental	Calculated	Diff.%
$Sr_4Al_{14}O_{25}$ (300K)	[7]	a(Å)	24.7451	25.103094	1.45
		b(Å)	8.4735	8.595316	1.44
		c(Å)	4.8808	4.933321	1.08
$Sr_2Al_6O_{11}$ (300K)	[8]	a(Å)	21.9140	22.231366	1.45
		b(Å)	4.8843	4.947937	1.30
		c(Å)	8.4039	8.508724	1.25
$Sr_3Al_2O_6$ (300K)	[9]	a(Å)	15.8556	15.949574	0.59
		b(Å)	15.8556	15.949574	0.59
		c(Å)	15.8556	15.949574	0.59
$Sr_9Al_6O_{18}$ (300K)	[10]	a(Å)	15.8476	15.949550	0.64
		b(Å)	15.8476	15.949550	0.64
		c(Å)	15.8476	15.949550	0.64
$Sr_7Al_{12}O_{25}$ (300K)	[11]	a(Å)	17.9100	18.355195	2.49
		b(Å)	17.9100	18.355195	2.49
		c(Å)	7.160000	6.931778	-3.19
$SrAl_{12}O_{19}$ (300K)	[12]	a(Å)	5.6581	5.640638	-0.31
		b(Å)	5.6581	5.640638	-0.31
		c(Å)	21.7776	21.917942	0.64
$SrAl_4O_7$ (300K)	[13]	a(Å)	13.0389	13.162647	0.95
		b(Å)	9.0113	9.160527	1.66
		c(Å)	5.5358	5.559149	0.42
		β/graus	106.7000	106.987196	0.27
$Sr_{10}Al_{16}O_{19}$ (300K)	[14]	a(Å)	34.5820	34.722108	0.41
		b(Å)	7.8460	7.910204	0.82
		c(Å)	15.7480	15.826944	0.50
		β/graus	103.6800	103.499167	-0.17
$SrAl_2O_4$ (monoclinic) (300K)	[15]	a(Å)	8.4470	8.442699	-0.05
		b(Å)	8.8160	9.033006	2.46
		c(Å)	5.1630	5.229848	1.29
		β/graus	93.4200	92.572269	-0.91
$SrAl_2O_4$ (hexagonal) (1073K)	[16]	a(Å)	8.9260	9.070489	1.62
		b(Å)	8.9260	9.070489	1.62
		c(Å)	8.4985	8.513597	0.18

Table 3. Lattice energies calculated at 0K and 300K and lattice energy per ion for each of the strontium aluminate phase.

Compoud	Lattice energy (eV)	Lattice Energy (eV) per íon	Lattice energy (eV)	Lattice Energy (eV) per íon
		0K		300K
$SrAl_2O_4$(monoclinic)	-192.77	-27.54	-192.39	-27.48
$SrAl_2O_4$(hexagonal)	-192.77	-27.54	-192.37	-27.48
$SrAl_4O_7$	-350.28	-29.19	-349.52	-29.13
$Sr_4Al_{14}O_{25}$	-1245.10	-28.96	-1242.45	-28.89
$Sr_3Al_2O_6$	-262.06	-23.82	-261.61	-23.78
$Sr_{10}Al_6O_{19}$	-819.77	-23.42	-818.53	-23.39
$Sr_9Al_6O_{18}$	-786.19	-23.82	-784.82	-23.78
$SrAl_{12}O_{19}$	-983.4	-30.73	-981.15	-30.66
$Sr_2Al_6O_{11}$	-544.03	-28.63	-542.81	-28.57
$Sr_7Al_{12}O_{25}$	-1167.04	-26.52	-1162.31	-26.42

3.2. Defect calculations

Defects were modelled using the Mott–Littleton approximation [22], in which a spherical region of the lattice surrounding the defect (region I) is treated explicitly, with all interactions being considered, and more distant parts of the lattice (region II) are treated using a continuum approach. A further division of the region II in region II(a) and II(b) are necessary to accommodate the distortions of the lattice induced by the defect. In region II(a) all displacements of the ions are calculated considering an harmonic approximation. Region II(b) is treated as a continuum dielectric media since the influence of the defect is negligible. Consistent cut-off radii of 10 and 14 Å have been used for regions I, and II (a) respectively. All this approximations are embodied in the GULP code.

As for the intrinsic defect (Frenkel, Schottky and others) standard defect reactions have been devised and they are listed in table 4. Basic defect formation energies were calculated, and used to evaluate the energies of defect reactions involved in the intrinsic disorders.

Table 4. Defect reactions used to compute the energies of the intrinsic defects for all Sr-Al-O crystalline systems.

Defect type	reactions
Frenkel defect	$Sr_{Sr} \rightarrow V''_{Sr} + Sr_i^{\bullet\bullet}$
	$Al_{Al} \rightarrow V'''_{Al} + Al_i^{\bullet\bullet\bullet}$
	$O_O \rightarrow V_O^{\bullet\bullet} + O_i$
Schottky defect	$xSr_{Sr} + yAl_{Al} + zO_O \rightarrow xV''_{Sr} + yV'''_{Al} + zV_O^{\bullet\bullet} + Sr_xAl_yO_z$
Anti-Shottky	$Sr_xAl_yO_z \rightarrow xSr_i + yAl_i + zO_i$
Pseudo-Schottky	$Sr_{Sr} + O_O \rightarrow V''_{Sr} + V_O^{\bullet\bullet} + SrO$
	$2Al_{Al} + 3O_O \rightarrow 2V'''_{Al} + 3V_O^{\bullet\bullet} + Al_2O_3$

4. Results and discussions

Computer simulations are an ideal way to approach intrinsic disorder in these complex systems because each defect can be treated separately and systematically. In strontium aluminates, vacancy and interstitial formation energies are calculated for each of the possible species. From these quantities, the energies per defect for the various possible types of disorder may be obtained.

In Table 5 all formation energies for the vacancy defects are displayed. It should be noticed that all possible non equivalent sites were considered for each material. In table 6(a), the formation energies for Sr, Al or O interstitials are shown for all 9 crystalline structures. In table 6(b) the interstitial positions used to calculate the previous values are shown.

Using the reactions presented in table 4 with values in tables 3, 5 and 6(a), the Schottky, pseudo-Schottky, anti-Schottky and Frenkel ddefect energies were calculated and this values are given in table 7. It should be pointed that only the lowest defect energy in each case were considered among all possible combinations of the values in tables 5 and 6(a). Also, the values quoted in table 7 were normalized by the number of basic defects forming the intrinsic defect, e.g., the Frenkel energies were divided by 2, Al_2O_3 pseudo-Schottky energies were divided by 5, and so on. The values in table 7 were computed considering that the basic defects involved in a specific intrinsic defect are not bound meaning that each constituent of the defect are formed separately in the lattice.

Table 5. Formation energy of all vacancy defect at non equivalent site.

$Sr_{10}Al_6O_{19}$		$Sr_2Al_6O_{11}$		$Sr_3Al_2O_6$	
Defect	Energy(eV)	Defect	Energy(eV)	Defect	Energy(eV)
V_{Sr1}	18.96	V_{Sr1}	19.17	V_{Sr1}	19.29
V_{Sr2}	18.46	V_{Sr2}	18.83	V_{Sr2}	17.61
V_{Sr3}	18.62	V_{Al1}	59.36	V_{Sr3}	18.00
V_{Sr4}	18.90	V_{Al2}	56.69	V_{Sr4}	17.84
V_{Sr5}	19.13	V_{Al3}	56.88	V_{Sr5}	18.80
V_{Sr6}	18.79	V_{Al4}	55.35	V_{Sr6}	19.73
V_{Sr7}	18.86	V_{Al5}	57.29	V_{Al1}	60.73
V_{Sr8}	18.67	V_{O1}	22.32	V_{Al2}	59.19
V_{Sr9}	19.10	V_{O2}	24.79	V_{O1}	23.37
V_{Al1}	58.82	V_{O3}	22.14	V_{O2}	23.19
V_{Al2}	57.76	V_{O4}	23.40	V_{O3}	23.00
V_{Al3}	58.10	V_{O5}	22.22	V_{O4}	21.87
V_{Al4}	58.09	V_{O6}	22.68	V_{O5}	21.89
V_{Al5}	58.46	V_{O7}	24.25	V_{O6}	22.85
V_{Al6}	59.98	$Sr_4Al_{14}O_{25}$		$SrAl_2O_4$(hex)	
V_{O1}	20.90	Defect	Energy(eV)	Defect	Energy(eV)
V_{O2}	22.41	V_{Sr1}	18.77	V_{Sr1}	19.38
V_{O3}	21.32	V_{Sr2}	19.40	V_{Sr2}	20.04
V_{O4}	21.15	V_{Al1}	55.63	V_{Al1}	56.66
V_{O5}	21.25	V_{Al2}	55.49	V_{Al2}	57.83
V_{O6}	22.02	V_{Al3}	55.44	V_{O1}	23.39
V_{O7}	21.54	V_{Al4}	56.90	V_{O2}	24.31
V_{O8}	22.38	V_{Al5}	59.33	V_{O3}	23.00
V_{O9}	22.07	V_{Al6}	56.65	V_{O4}	24.27
V_{O10}	22.47	V_{O1}	22.72	$SrAl_4O_7$	
V_{O11}	21.70	V_{O2}	23.50	Defect	Energy(eV)
V_{O12}	19.19	V_{O3}	24.49	V_{Sr1}	19.78
V_{O13}	21.10	V_{O4}	26.89	V_{Al1}	56.32
V_{O14}	21.70	V_{O5}	22.33	V_{Al2}	55.68
V_{O15}	21.81	V_{O6}	22.48	V_{O1}	23.60
V_{O16}	20.76	V_{O7}	25.18	V_{O2}	23.36
V_{O17}	21.41	V_{O8}	23.06	V_{O3}	25.25
V_{O18}	21.35	V_{O9}	24.62	V_{O4}	24.12
V_{O19}	20.88				
$Sr_9Al_6O_{18}$		$SrAl_2O_4$(mono)		$SrAl_{12}O_{19}$	
Defect	Energy(eV)	Defect	Energy(eV)	Defect	Energy(eV)
V_{Sr1}	19.29	V_{Sr1}	19.48	V_{Sr1}	19.41
V_{Sr2}	17.61	V_{Sr2}	19.68	V_{Al1}	54.70
V_{Sr3}	18.00	V_{Al1}	57.78	V_{Al2}	54.84
V_{Sr4}	17.84	V_{Al2}	57.73	V_{Al3}	54.18
V_{Sr5}	18.80	V_{Al3}	56.81	V_{Al4}	54.49
V_{Sr6}	19.73	V_{Al4}	57.61	V_{Al5}	58.28
V_{Al1}	60.73	V_{O1}	23.54	V_{O1}	23.99
V_{Al2}	59.19	V_{O2}	24.52	V_{O2}	22.75
V_{O1}	23.37	V_{O3}	24.61	V_{O3}	22.64
V_{O2}	23.19	V_{O4}	24.54	V_{O4}	24.68
V_{O3}	23.00	V_{O5}	24.17	V_{O5}	23.36
V_{O4}	21.87	V_{O6}	24.64		
V_{O5}	21.89	V_{O7}	23.61		
V_{O6}	22.85	V_{O8}	23.10		

Table 6(a). Formation energies of the interstitial defects for all strontium aluminate systems.

Compoud					Defect Energy(eV)				
Def. type	$SrAl_2O_4(m)$	$SrAl_2O_4(h)$	$SrAl_4O_7$	$Sr_4Al_{14}O_{25}$	$Sr_3Al_2O_6$	$Sr_{10}Al_6O_{19}$	$Sr_9Al_6O_{18}$	$SrAl_{12}O_{19}$	$Sr_2Al_6O_{11}$
Sr_i	-12.09	-12.39	-12.15	-12.34	-14.92	-11.04	-10.00	-6.60	-11.74
Al_i	-44.31	-44.25	-42.80	-39.59	-45.25	-45.61	-45.39	-43.96	-43.04
O_i	-14.43	-15.29	-18.52	-14.86	-10.53	-15.18	-14.60	-15.90	-14.48

Table 6(b): Interstitial positions used for calculating the interstitial formation energies.

	Intersticial position(fractional)		
Compoud	x	y	z
$SrAl_2O_4$(monoclinic)	0.3680	0.1580	0.2945
$SrAl_2O_4$(hexagonal)	0.3320	0.3370	1.0000
$SrAl_4O_7$	0.0000	0.4050	0.1250
$Sr_4Al_{14}O_{25}$	0.2500	0.5000	0.7965
$Sr_3Al_2O_6$	0.1145	0.8705	0.7437
$Sr_{10}Al_6O_{19}$	1.0000	0.9810	0.5671
$Sr_9Al_6O_{18}$	0.2500	0.0000	0.0000
$SrAl_{12}O_{19}$	0.3333	0.1667	0.1250
$Sr_2Al_6O_{11}$	0.1804	0.0604	0.0000

Table 7. Solution energies of the intrinsic defects for the Sr-Al-O systems.

Compoud					Defect Energy(eV)				
Defect type	$SrAl_2O_4(h)$	$SrAl_2O_4(m)$	$SrAl_4O_7$	$Sr_4Al_{14}O_{25}$	$Sr_3Al_2O_6$	$Sr_{10}Al_6O_{19}$	$Sr_9Al_6O_{18}$	$SrAl_{12}O_{19}$	$Sr_2Al_6O_{11}$
Frenkel									
Sr	**3.70**	**3.50**	3.82	**3.22**	**1.35**	3.71	3.81	6.41	3.55
Al	6.25	6.21	6.44	7.93	6.97	6.08	6.90	5.11	6.16
O	4.34	3.86	**2.42**	3.74	5.67	2.01	3.64	**3.37**	3.83
Pseudo-Schottky									
SrO	4.08	3.98	4.36	3.34	2.53	**1.61**	**2.53**	3.81	**3.27**
Al_2O_3	4.94	4.82	4.64	3.93	5.15	2.97	5.15	3.65	3.81
Schottky	4.68	4.56	4.65	3.82	3.67	2.17	3.67	3.63	3.65
Anti-Schottky	4.91	4.39	7.74	6.28	5.78	4.21	4.88	4.60	5.42

Results presented in table 7 reveals that the 9 crystalline systems can be divided in 3 groups according to the preferred intrinsic disorder. Group I contains both phases of $SrAl_2O_4$, $Sr_4Al_{14}O_{25}$ and $Sr_3Al_2O_6$ where the Sr Frenkel disorder gives the lowest energies. In group II are the systems where the O Frenkel defect is more likely to occur and this group is formed by the $SrAl_4O_7$ and $SrAl_{12}O_{19}$. Finally, $Sr_{10}Al_5O_{19}$, $Sr_9Al_6O_{18}$ and $Sr_2Al_6O_{11}$ form group III, where the pair of Sr and O vacancies (pseudo-Schottky type defect) are the most favourable defect.

For the $SrAl_{12}O_{19}$ case, our predictions agree with the results obtained by Jae-Gwan Park and Cormack [23]. Experimental results by Beauger et al [24] showed that during the synthesis of $SrAl_2O_4$, the $Sr_3Al_2O_6$ is also formed as a marginal phase. The authors attributed that to the presence of strontium vacancies (V_{Sr}), and hence oxygen vacancies (V_O), in the main $SrAl_2O_4$ phase leading to a stoichiometric deviation from the $SrAl_2O_4$ phase forming a region rich with Sr and O that can give rise to the undesirable $Sr_3Al_2O_6$ phase. They also showed that their thermoluminescence (TL) measurements carried out for the stoichiometric and nonstoichiometric samples of $SrAl_2O_4$: Eu^{2+} [24] indicate that Sr and O vacancies could be present. This agree with the new phosphorescence mechanism proposed of Clabau et al. proposed for $SrAl_2O_4$:Eu^{2+}, Dy^{3+}, B^{3+}[1].

5. Conclusions

A new set of potential parameters were fitted in order to reproduce all the experimental crystalline structure available for the Sr-Al-O compounds and the potential parameters were able to reasonably reproduce all the crystalline structures within 3%. This potential set was then used to model the intrinsic defects of the strontium aluminates compounds. According to the obtained energy, we found that in $Sr_2Al_6O_{11}$, $Sr_9Al_6O_{18}$ and $Sr_{10}Al_6O_{19}$ SrO pseudo-Schottky defect is more likely to occur. In $SrAl_4O_7$ and $SrAl_{12}O_{19}$ the lowest energy was obtained for the oxygen Frenkel defect. On the other hand, in $SrAl_2O_4$ (monoclinic), $SrAl_2O_4$ (hexagonal), $Sr_3Al_2O_6$, and $Sr_4Al_{14}O_{25}$ the Strontium Frenkel defect is the preferred intrinsic defect.

Acknowledgements

Reference

[1] Clabau F, Rocquefelte X, Jobic S, Deniard S, Whangbo M-H, Garcia A, Mercier T Le 2005 *Chem. Mater.* **17** 3904-3912.

[2] Lin Y, Tang Z, Zhang Z 2001 *Materials Letters* **18** 5114.

[3] Chang C, Mao D, Shen J, Feng C 2003 *J. Alloys Compd.* **348** 224.

[4] Zhong R, Zhang J, Zhang X, Lu S, Wang X-J 2006 *Journal of Luminescence* **119–120** 327-331.

[5] Shionoya S, Yen W 1999 *Phosphor Handbook*, CRC Press, New York.

[6] McKeever S 1988 *Thermoluminescence of Solids*, Cambridge Press University, Cambridge.

[7] Wang D, Wang M-Q, Lu G-G 1999 *Journal of Materials Science* **34** 4959-4964.

[8] Takeda T, Takahashi T, Takeda K, Takahashi T, Uheda K, Takizawa K, Takeda H 2004 *Journal of the Japan Society of Powder Metallurgy* **49** 1128-1133.

[9] Chakoumakos B C, Lager G A, Fernandez-Baca J A 1992 *Acta Crystallographica C* **48** 414-419.

[10] Alonso J A, Rasines I, Soubeyroux J L 1990 *Inorganic Chemistry* **29** 4768-4771.

[11] Nevskii N N, Glasser L D, Ilyukhin V V, Belov N V 1979 *Kristallografiya* **24** 161-166.

[12] Park J-G, Cormack A N 1996 *Journal of Solid State Chemistry* **121** 278-290.

[13] Lindop A J, Goodwin D W 1972 *Acta Crystallographica* **28** 2625-2526.

[14] Kahlenberg V 2003 *Materials Research Bulletin* **37** 715-726.

[15] A. R. Schulze, Hk. Mueller-Buschbaum, Zeitschrift fuer Anorganische und Allgemeine Chemie 475 (1981) 205-210.

[16] Fukuda K, Fukushima K 2005 *Journal of Solid State Chemistry* **178** 2709-2714.

[17] Gale J D 1997 *J. Chem. Soc., Faraday Trans.* **93** 629.

[18] Dick B J, Overhauser A W 1958 *Phys. Rev.* **112** 90.

[19] Sandes M J, Leslie M, Catlow C R A 1984 *J. Chem. Soc. Chem. Commun* 1271.

[20] LeSar R, Najafabati R, Srolovitz D J 1991 *J. Chem. Phys.* **94** 5090–5097.

[21] Montes P J R, Valerio M E G, Azevedo G M 2008 *Nuclear Instruments and Methods in Physics Research B* **266** 2923-2927.

[22] Mott N F, Littleton M J 1938 *Trans. Farady Soc.* **34** 485.

[23] Park J-G, Cormack N A 2000 *Korean J. Crystallography* **11** 176-181.

[24] Beauger, *Thesis C, Université de Nice* 1999 Nice, France.